Revised manuscript (unmarked)
Click here to view linked References

Application of Activated Carbon Fiber as the Substrate in Biofiltration-Nanofiltration Process Treating Surface Water

Cong Ma[a,b], Qingqiang Dou[a,b], Lei Xu[b*], Samia Saleem[b], Nigel Graham[c], Wenzheng Yu[b*]

[a] State Key Laboratory of Advanced Separation Membrane Materials, School of Environmental Science and Engineering, Tiangong University, Tianjin 300387, China

[b] Key Laboratory of Drinking Water Science and Technology, Research Centre for Eco-Environmental Sciences, Chinese Academy of Sciences, Beijing, 100085, China

[c] Department of Civil and Environmental Engineering, Imperial College London, South Kensington Campus, London SW7 2AZ, United Kingdom

Abstract: This study has evaluated different types of carbon fiber (CF) biofiltration media in terms of their efficiency in mitigating nanofiltration (NF) fouling and their ability to remove natural organic matter (NOM) and disinfection by-product formation potential (DBPFP). Compared to direct NF, a combined CF biofiltration-NF system enhanced dissolved organic carbon and DBPFP removal by up to 32.6% and 39.1%, respectively, achieving final removal rates of 78.45% and 85%. Furthermore, this combined system reduced irreversible NF fouling by up to 44.5%. Specifically, activated carbon fiber (ACF) exhibited a greater tendency to remove low-molecular-weight organics, thus achieving greater performance. Microbial sequencing and correlation analyses further indicated that the microbial communities were significantly influenced by the physicochemical properties of the CF, such as microporosity, electrical resistance, and

surface functional groups. Pore size distribution and carboxyl content were shown to promote the enrichment of dominant species such as *Pseudomonadota*, *Chloroflexota*, and *Bacillota*. This led to a higher expression of fatty acid metabolism and the citric acid cycle, contributing to the degradation and removal of DOM and DBPFP. Overall, this study demonstrates the promising potential of applying CF as a biofiltration substrate to improve subsequent NF processes, and achieving greater water treatment performance overall by the combined CF-NF process.

Keywords: Activated carbon fiber; Low-molecular-weight organics; Biofiltration; Nanofiltration; Microbial metabolism

1. Introduction

In response to increasing water scarcity and declining source water quality, more effective and sustainable technologies are crucial and urgent [1]. With respect to safe drinking water supplies, previous studies have shown that natural organic matter (NOM) in raw waters can form disinfection byproducts (DBPs) during chlorination, with potential links to bladder and colorectal cancers [2, 3]. Therefore, removing NOM more effectively is essential for mitigating adverse effects on treated waters and enhancing the performance of treatment processes, such as membrane filtration.

Biofiltration is a cost-effective and environmentally friendly water treatment process. Common filtration media include granular activated carbon, anthracite, ceramic materials, and

sand [4]. Similar to conventional filter media, carbon fiber (CF) is a porous material and represents the third generation of carbon products with a fibrous structure. Through activation, activated carbon fiber (ACF) is produced, which has a fibrous structure, numerous micropores, excellent volumetric capacity, and a larger specific surface area. Compared to granular activated carbon, ACF's micropores are primarily concentrated on the material surface, which results in faster adsorption rates, shorter adsorption paths, and reduced resistance to adsorption [5]. Previous studies have demonstrated that ACF is highly effective in adsorbing organic pollutants, including NOM and pharmaceutical compounds [5, 6]. Additionally, ACF has been shown to be a suitable carrier for biodegradation processes [7]. Therefore, it is proposed that ACF could be a superior choice as a biofiltration media to enhance treatment efficiency.

Previous research has shown that activated carbon made from different materials can alter microbial community structure and microbial activity, with pore size distribution playing a key role in biofiltration performance by influencing the abundance of key microbial species [8-10]. Moreover, surface acidic functional groups have been found to affect the adsorption properties of the medium, influencing microbial aggregation [11]. Despite these findings, the role and impact of ACF as a biofiltration medium for the removal of dissolved organic matter (DOM) and disinfection byproduct formation potential (DBPFP) from surface water remain unexplored. Furthermore, there is limited research on the synergistic effects of the physicochemical properties of the filter media on microbial metabolism related to NOM.

Previously, combining biofiltration with subsequent nanofiltration (NF) has been used to

further reduce organics and improve final treated water quality [12]. However, the impact of CF as biofiltration media on subsequent NF performance remains unclear, especially in the complex and variable organic environments of surface waters. Therefore, this study explores a combined biofiltration and NF process to treat real surface water, using CF as the biofilter media. The primary objectives are to investigate the impact of CF on NOM removal and subsequent NF performance from a mechanistic perspective. Particular emphasis is placed on understanding the reciprocal effects between the physicochemical properties of CF, microbial metabolism, and NOM removal. Overall, this work aims to deepen the understanding of CF-based biofiltration and provide valuable insights for its practical application in treating surface water for potable supplies.

2. Materials and Methods

2.1. System setup and operation

A parallel bench-scale up flow biofiltration system, based on three quartz glass columns (height: 400 mm, inner diameter: 25 mm), was established to treat surface water from a local lake (Olympic Park, Beijing, China)(SI, table S1). A schematic diagram is shown in the Supplementary Information (Fig. S1). Briefly, three types of CF media were cut into 1×1 cm square pieces and packed into their respective columns to ensure a uniform media volume in each (approximate depth of 0.5 mm). CF and ACF (ACF-1 and ACF-2) materials were purchased from Beierge Activated Carbon Fiber Co., Ltd. (Nantong, China). Raw water was fed to the

bottom of the biofilters by a multi-channel peristaltic pump at a fixed flow rat, resulting in an upwards flow through the column corresponding to a hydraulic retention time (HRT) of approximately 24 h. The flow discharged from the top of each column and was collected in storage bottles for subsequent analysis and application to the Nanofiltration unit.

2.2. Water quality analysis and fouled membrane characterizations

Water samples were collected from the Olympic Park lake and transported to the laboratory for storage prior to use. The samples were filtered through 0.45 μm syringe filters prior to analysis, as follows. The dissolved organic carbon (DOC) concentration was determined using a total organic carbon analyzer (TOC-Vwp, Shimadzu, Japan). The fluorescence intensity of fluorescent organics was characterized using 3D excitation-emission matrix (EEM) fluorescence spectrophotometry (F-4600 FL, HITACHI, Japan). Specific fluorescent compounds were quantified using parallel factor analysis (PARAFAC) and fluorescence region integration. UV-visible absorbance spectra were obtained using a UV-visible spectrometer (UV-2600, Shimadzu, Japan) over a wavelength range of 200-800 nm. In addition, the molecular weight (MW) distribution of dissolved organic matter (DOM) was determined by a high-performance liquid chromatography (HPLC) system (Waters, USA) coupled with a size exclusion chromatography (SEC) column (Phenomenex, BioSep 5 mm, SECs3000). Surface functional groups of lyophilized samples and NF membranes were characterized by Attenuated Total Reflection Fourier Transform Infrared (ATR-FTIR) spectroscopy (Spectrum Two, PerkinElmer), scanning from 4000-400 cm^{-1} at a 4 cm^{-1} resolution. The chemical bonding composition of CF and lyophilized

samples was analyzed using X-ray Photoelectron Spectroscopy (XPS) (Thermo Scientific 250Xi).

2.3. Nanofiltration tests and DBPFP measurements

A commercial polyamide (PA) NF membrane (NF90, RisingSun Membrane Technology (Beijing) Co., Ltd.) was used in this work. Filtration tests were conducted at room temperature using a laboratory-scale dead-end filtration setup (Millipore, Amicon 8400, USA) with an effective membrane area of 45.34 cm^2 at a pressure of 4 bar, supplied by ultrapure N_2. The membrane flux was determined indirectly by automatically recording the weight of the filtered effluent by a digital balance connected to a computer (Figure S1). Three consecutive filtration cycles were performed, each with a feed water (biofilter effluent) volume of 100 mL. Backwashing was performed by inverting the contaminated membrane and filtering 10 mL of deionized (DI) water at 1 bar. To eliminate the influence of membrane impurities, new membranes were soaked in deionized water for more than 24 h, and only membranes with a similar initial filtration flux were selected for experiments.

The DBPFP of biofiltration and NF effluents were determined after chlorination, in terms of the commonly detected trihalomethanes (THMs) and haloacetic acids (HAAs), to assess DOM conversion and the ability of the treatment methods to eliminate DBP precursors, as detailed in the SI (Text S2).

2.4. Characterizations of the CFs

The specific surface area and pore structure of the CF media were characterized by a fully

automated specific surface and porosity analyzer (Micromeritics ASAP 2460, USA) via the Brunauer-Emmett-Teller (BET) method. X-ray photoelectron spectroscopy (XPS, Thermo Scientific K-Alpha, USA) was used to investigate the specific forms of functional groups on the CF surfaces. Quantification of acidic functional groups on the CF surfaces was achieved by the Boehm titration method (SI, Text S1) [13].

2.5. Microbial diversity and metabolism

At the end of the experiment, CF pieces from each column were sampled and stored in sterile centrifuge tubes at -20°C for DNA extraction and 16S rRNA analysis. After high-throughput sequencing, the resulting data were filtered, and all samples were normalized to 33,974 sequences. Microbial community structure and diversity were processed and analyzed using the Majorbio Cloud Platform. To assess differences between bacterial communities, principal coordinate analysis (PCoA) and linear discriminant analysis (LDA) effect size (LEfSe) were performed. LEfSe (with an LDA score threshold of 4) was used to identify species that were significantly different between columns. PICRUSt2 was used to predict the potential functions of the bacteria based on level 3 of the Kyoto Encyclopedia of Genes and Genomes (KEGG) database. The raw sequencing data were deposited in the Sequence Read Archive (SRA) database of the National Center for Biotechnology Information (NCBI) under accession number PRJNA131025.

3. Results and Discussions

3.1 Influences of different CFs on DOM removal via biofiltration

The DOM removal rates for the biofilters over the course of the experiment are summarized in Fig. 1a. The entire operational period, 122 d, can be divided into two stages. During the first stage, the DOM removal rate was the highest, primarily driven by adsorption, and this stage was non-stationary. As the treatment process progressed, the removal efficiency gradually decreased due to the saturation of adsorption sites and eventually stabilized [14]. In the second stage, the DOM removal was sustained by both biodegradation and adsorption, reaching an approximate steady-state, with biodegradation driven by bacterial metabolic activity [15]. For stage II, the DOM removal of CF, ACF-1, and ACF-2 showed significant differences, with average removal rates of approximately 13.7%, 22.6%, and 43.2%, respectively.

Analysis of the total fluorescence intensities of the biofilter effluents indicated that ACF-2 had the best performance in removing fluorescent organics (SI, Fig. S3). This can be attributed to the combined effects of adsorption and biodegradation by microorganisms that were acclimated over the long-term operation [16, 17]. Specifically, three fluorescent components were identified through PARAFAC analysis, as shown in Fig. 1b. Among these, C1 exhibited excitation and emission wavelengths similar to those of microbial humic-like DOM [18-20], while C2 and C3 were found to resemble protein-like components and terrestrial humus-like DOM derived from soil and terrestrial plants, respectively, with excitation and emission similarity scores greater than 0.95 [19, 21-23]. Compared to the raw water, ACF-2 achieved the greatest reduction of C2 and C3, of 47.9% and 59.2%, respectively. The C1 component was

effectively removed by all three biofilter systems, with ACF-2 achieving a 43.8% improvement over ACF-1 (overall removal 65.4% vs. 45.4%) (Fig. 1c).

Figure 1

3.2 MW distribution of DOM and microbial derived biopolymers

The changes in the MW distribution of organics in the raw water and the corresponding biofilter effluents are summarized in Fig. 2a. The results show that medium-sized organics (1-10 kDa) were the dominant fraction in all the samples, with ACF-2 performing the best in removing organics within this range. Additionally, as shown in Fig. 2b, the removal rates of DOM in the MW range of 0–800 Da were approximately 160% (ACF-1) and 250% (ACF-2) greater than CF (27.1%), achieving removal rates of 71.3% and 96.5%, respectively. For DOM in the MW range of 800–1400 Da, the removal rates were approximately 140% (ACF-1) and 270% (ACF-2) greater than CF. These results demonstrate that ACF was superior in removing low-molecular-weight (LMW) organic compounds, likely due to the abundant micropores in ACF, which facilitate the adsorption and biodegradation of LMW organics [24]. Interestingly, the peak of CF around 4000 Da was greater than that of ACF-1. It was found that, compared to ACF-1, both CF and ACF-2 possessed richer amounts of phenolic hydroxyl groups (as will be shown in later sections), enabling the formation of multiple hydrogen bonds with carboxyl or carbonyl functional groups prevalent in medium-molecular-weight (MMW) humic substances, thus enhancing their removal [25, 26]. The content of microbially derived macromolecular

DOM, or biopolymers (represented by polysaccharides and proteins), in the raw water and biofilter effluents was further explored (Fig. 2c, d). The results show that biofiltration reduced the polysaccharide and protein content to varying degrees. ACF-2 achieved removal rates of approximately 46.4% for polysaccharides and 91% for proteins, representing 3.3 times and 3 times improvement over CF (10.6% and 30.3%), respectively. The EEM results also indicated that protein components in the effluents differed due to microbial degradation and matrix adsorption, with fluorescent protein components significantly reduced by the ACF-2. Previous studies have shown that extracellular enzymes secreted by microorganisms (e.g., proteases, amylases, cellulases) can break down large molecules of polysaccharides and proteins into smaller organic molecules [27]. Furthermore, microbial metabolism (respiration or anabolism) can convert macromolecular DOM into energy and cellular matter [28], which reveals more efficient biodegradation in the ACF-2 system.

Figure 2

3.3 Impact of biofiltration on NF

Organic matter in the biofiltration effluent was further analyzed by XPS to obtain detailed information about its chemical bonding. In all profiles (Fig. 3a), the C 1s peak can be deconvoluted into three main bonding peaks. The peak at C1 is attributed to C-C/C-H, which is mainly derived from hydrocarbon compounds, including the side chains of polysaccharides,

amino acids, and lipids [29]. The peak at C2 is associated with C-O/C-N bonds in amide, alcohol, or ether amine groups found in proteins and polysaccharides. The weak peak at C3 is attributed to RCOOH/O=CO-R, such as the carboxyl or ester groups of carboxylates and saccharides [30]. Compared to the DOM in the raw water, the proportion of C2 components in the effluent from CF, ACF-1, and ACF-2 increased by 5.82%, 1.39%, and 7.31%, respectively, while the proportion of C1 components decreased. This may be attributed to extracellular hydrolases in the biofilm breaking down macromolecular polysaccharides and proteins into corresponding amides or monosaccharides [31]. This enhanced functional expression likely results in a stronger polysaccharide degradation capacity in the ACF-2 system, leading to a greater reduction in C1 components. Furthermore, the reduction in C1 components across all three systems corresponds to the decrease in protein-like components observed in the EEM results. In the O 1s spectra, the O1 peak corresponds to C=O bonds from carboxylate, carbonyl, ester, or amide compounds; O2 is attributed to compounds such as alcohols, aldehydes, or sugars (RHC(OH)(OR)/C-O-H/C-O-C); and O3 is attributed to nitrogen oxides (NOx). The reduction in O2 content across all biofiltration systems may originate from the mineralization and degradation of substances such as humic compounds and sugars [32].

Regarding the impact of biofiltration on subsequent NF, all three systems reduced membrane fouling to varying degrees compared to the raw water (Fig. 3b). Among them, pretreatment with the ACF-2 biofilter most significantly mitigated fouling, increasing the final membrane flux by approximately 16.9% relative to the raw water filtration. NF membrane fouling

220 can be categorized as reversible or irreversible [20]. When filtering raw water, irreversible
221 fouling accounted for 43.17% of the total fouling. Due to the dual effects of biodegradation
222 and adsorption on NOM, the irreversible fouling of the NF membrane when filtering the efflu-
223 ent from CF, ACF-1, and ACF-2 was reduced by approximately 15.6%, 22.3%, and 44.5%,
224 respectively. Previous research has indicated that biopolymer concentration is positively cor-
225 related with total membrane resistance. Biopolymers exhibit a high degree of adhesion, and
226 their adherence to the membrane surface increases filtration resistance [33]. At the same time,
227 LMW organic compounds can result in NF membrane pore blockage, leading to irreversible
228 fouling [34]. Therefore, the biopolymers and LMW compounds removed by biofiltration are
229 key factors contributing to the mitigation of different types of membrane fouling. It was ob-
230 served that the CF removed only about 33% of the LMW organics, and its removal of polysac-
231 charides and proteins was also significantly lower than that of ACF-2 (by approximately 22.8%
232 and 33.2%, respectively). Consequently, the ACF-2 system can significantly reduce irreversible
233 membrane fouling, which is a key contributor to mitigating overall membrane fouling. Further-
234 more, the reduction in irreversible fouling can also be attributed to a fundamental change in
235 fouling-layer structure. Biofiltration preferentially degrades high-affinity protein-like com-
236 pounds and long-chain fatty acids, resulting in a more porous, granular deposit layer on the NF
237 membrane [35]. This transformation, driven by DOM biotransformation and enhanced electro-
238 static repulsion between transformed organics and the membrane surface, reduces chemical

239 anchoring of foulants, thereby enabling more effective flux recovery through simple hydrody-
240 namic cleaning.

241 The schematic in Fig. 3c illustrates the overall NF process, where high-molecular-weight
242 organics (such as humic acids, polysaccharides, and proteins) are retained primarily by the size
243 exclusion and Donnan effects of the NF membrane [36]. These retained substances accumulate
244 on the membrane surface, forming a gel layer. This layer acts as a secondary barrier, increasing
245 permeation resistance and consequently reducing flux [37]. Simultaneously, the removal of
246 LMW organics (such as carboxylates and sugar alcohols) via the preceding biofiltration process
247 reduces membrane pore blockage, thereby mitigating flux decline. In addition, the deproto-
248 nated, negatively charged functional groups on the polyamide NF membrane surface promote
249 the removal of negatively charged dissolved organics via electrostatic repulsion [38-40]. This
250 phenomenon, combined with the XPS data showing that ACF-2 effluent contained more oxi-
251 dized (and thus more electronegative) DOM, further explains the superior performance of the
252 ACF-2 pretreatment.

253 Contact angle tests were also conducted on the fouled NF membranes to evaluate the hy-
254 drophilicity of the accumulated foulant layer (Fig. 3d). Compared to the virgin NF membrane,
255 the contact angles of all fouled membranes decreased, suggesting an accumulation of hydro-
256 philic organic matter on the membrane surface [41]. The contact angle decreased most signifi-
257 cantly for the membrane fouled by raw water. In contrast, the contact angles of membranes

filtering the biofilter effluents were higher (i.e., less hydrophilic). Specifically, the contact angles for membranes filtering ACF-1 and ACF-2 effluents were approximately 14.7% and 20% higher, respectively, than that of the membrane fouled by raw water. This increase may be attributed to the removal of hydrophilic polysaccharide components via biofiltration [42], as ACF-1 and ACF-2 removed 32.1% and 46.4% of these components, respectively. Furthermore, because biofiltration removes a large amount of organic matter, there is less foulant build-up on the membrane surface, resulting in a contact angle closer to that of the virgin polyamide membrane [43].

Figure 3

3.4 Water quality analysis before and after NF

As shown in Fig. 4a, direct NF of the raw water resulted in a DOC removal rate of 59.17%. However, pretreatment with ACF-2 provided the greatest improvement, increasing the total DOC removal by 32.8% to a final rate of 78.45%. In comparison, the systems using ACF-1 and CF pretreatment achieved total removal rates of 65% and 62%, respectively. This difference likely stems from the biofiltration process altering the composition of the organic matter. As indicated by the XPS results, the proportion of oxygen-containing carbon (i.e., C2 and C3) progressively increased (from 30.46% in raw water to 36.09% after ACF-2 treatment). This results in an elevated average binding energy of carbon atoms within the DOM, enhancing its overall electronegativity [44]. Consequently, a greater amount of these more electronegative

278 organic compounds is removed by the NF membrane via electrostatic repulsion. Furthermore,
279 the ACF biofilter removes LMW organic compounds, which would be more likely to pass
280 through the membrane pores. The combination of these effects (increased electronegativity and
281 removal of LMW compounds) alters the DOM composition, leading to a higher overall reten-
282 tion rate by the NF membrane. EEM fluorescence spectroscopy also confirmed the positive
283 effect of biofiltration on removing fluorescent dissolved organic matter (FDOM) (Fig. 4b). The
284 ACF-2 system was the most effective, showing the highest removal of FDOM, including tyro-
285 sine-like (Region I), tryptophan-like (Region II), and fulvic/humic-like compounds (Regions
286 III and VI). As shown in Fig. 2b, the DOM in both raw water and biofiltration effluent was
287 dominated by molecules exceeding 1 kDa. This suggests that size exclusion is the primary
288 retention mechanism for the NF membrane [45, 46]. After NF, the intensities of all fluorescent
289 peaks were substantially reduced (Fig. 4c), which was consistent with the high removal rates
290 observed in the DOC and EEM analyses.

291 Previous studies have shown that trihalomethane formation potential (THMFP) is highly
292 influenced by hydrophobic DOM, whereas haloacetic acid formation potential (HAAFP) is
293 more dependent on the hydrophilic fraction [47]. In our system, the combination of standard
294 (non-activated) CF and NF reduced THMFP by 61.4%, which was primarily attributed to the
295 65.4% removal of DOC (Fig 4d). The ACF-2 and NF combination was most effective, increas-
296 ing the THMFP removal by 35.3% (compared to NF alone) to a total reduction of 83.1%. This

297 superior performance may be attributed not only to the high DOC removal but also to the mi-
298 crobial conversion of large hydrophobic organic molecules into small organic acids via aerobic
299 respiration, which inherently reduces THMFP [48]. Organic composition analysis indicated
300 that biofiltration altered the carbon bonding, significantly increasing the affinity of organic
301 molecules for water. This process makes them more water-soluble, thus enhancing the overall
302 hydrophilicity of the DOM [49, 50]. A calculation of the specific THMFP (per unit of DOC)
303 supports this: the value decreased from 69.6 μg/g in the raw water to 54.5 μg/g in the ACF-2
304 effluent, indicating a selective reduction in hydrophobic THM precursors. For HAAs, NF alone
305 achieved a 68% removal rate. This is likely due to the retention of hydrophilic DOC (which
306 serves as HAA precursors) on the NF membrane surface, a conclusion indirectly supported by
307 the increased hydrophilicity of the membrane after filtering raw water. In comparison, the ACF-
308 2 and NF combination was again the most effective treatment, achieving an 89.5% HAAFP
309 removal (while total DOC removal was 78.45%). This enhanced HAAFP reduction can be par-
310 tially ascribed to the microbial conversion of biopolymers and humic acids into small-molecule
311 organics, which are less likely to form HAAs [51]. Finally, calculating the specific HAAFP
312 (per unit of DOC) after NF treatment showed a 38.1% reduction, from 22 μg/g in the raw water
313 to 13.4 μg/g in the ACF-2 effluent. This indicates that the combined system effectively inter-
314 cepted more electronegative organic matter, including the hydrophilic HAA precursors.

315 **Figure 4**

316

3.5 Physical and chemical properties of CFs

To establish why the CF and ACFs exhibited different DOM removal performance, their physicochemical properties were first investigated. The pore properties of the CF/ACFs were evaluated in terms of N_2 adsorption-desorption isotherms at 77 K. As shown in Fig. 5a, both ACFs exhibited Type I isotherms [52]. The N_2 adsorption increased rapidly in the low-pressure region, indicating the presence of abundant micropores. In contrast, the N_2 adsorption capacity of the standard (non-activated) CF was poor, and a clear adsorption curve was not detected. The results shown in Fig. 5b summarize the pore volume and specific surface area of the ACFs, confirming that they contain abundant micropores, whereas the standard CF contained almost none. This explains the higher removal capability for LMW organics by the ACFs. The unique fibrous morphology and continuous pore channels of ACFs likely reduce mass transfer resistance, allowing LMW organics to diffuse rapidly to adsorption sites and achieve a rapid adsorption equilibrium [24]. The pore size distributions of the CF and ACFs are given in the SI (Fig. S4), where it can be seen that the poor adsorption performance of the CF yielded no detectable results. The DOM adsorption capacity of the ACFs was further evaluated using pseudo-first-order (Fig. S5) and pseudo-second-order (Fig. 5c) adsorption kinetics. The equilibrium adsorption capacities of ACF-2 and ACF-1 were 1.66 and 1.32 mg/g, respectively, while that of the CF was only 0.26 mg/g. Notably, ACF-2 exhibited a 10.7% greater micropore volume and a 10.1% larger specific surface area than ACF-1. However, the equilibrium adsorp-

tion capacity of ACF-2 for DOM was 25.7% greater than that of ACF-1, indicating that chemical adsorption differences also played a role. The surface acidic functional groups of the ACFs were subsequently quantified using Boehm titration (Fig. 5d). The total content of acidic functional groups on the ACF surfaces was found to be approximately twice that of the standard (non-activated) CF, a property that can favor the removal of hydrophilic organic compounds. Furthermore, the significantly higher concentration of electron-deficient carboxyl groups may also accelerate electron transfer and promote microbial activity following acclimation [53]. Their presence also lowers the electron-transfer barrier between microbial electroactive proteins and the material surface, thereby accelerating respiratory chain cycling and increasing metabolic rates.

Figure 5

3.6 Influence of CF and ACFs on microbial diversity and metabolism

Understanding the impact of different biofilters on microbial communities can further reveal the underlying mechanisms for the different DOM removal performances. Based on the Bray-Curtis distance and principal coordinates analysis (PCoA), significant differences in microbial community composition were observed for the different biofilters (Adonis, $R^2 = 0.8421$, $P = 0.001$) (Fig. 6a). Venn diagrams of amplicon sequence variants (ASVs) revealed variability among the three biofiltration systems, with unique ASVs accounting for 72.89%, 53.68%, and 56.13% of the total unique ASVs in CF, ACF-1, and ACF-2, respectively. Richness (Chao1)

and diversity (Shannon index) analyses show that ACF-2 had a higher richness and diversity than both ACF-1 and CF (Fig. 6c). At the phylum level, *Pseudomonadota* emerged as the most dominant phylum in the ACF-2 biofilter (34.4%), which was 1.2 times more abundant than ACF-1. *Pseudomonadota* is known for its ability to degrade polysaccharides [54], while *Chloroflexota* breaks down complex polymeric organic compounds into low molecular weight substances and mineralizes them [55], being 1.1 times more abundant in ACF-2 than in ACF-1. At the genus level (SI, Fig. S8), the abundance of several genera in ACF-2 was much greater than in the CF, including *Ignavibacterium* (average absolute abundance: 2.621 vs 0.971), *Ellin6067* (average absolute abundance: 2.956 vs 1.239), and *Pseudolabrys* (average absolute abundance: 2.612 vs 1.569). These microorganisms are adept at degrading organic matter [56, 57], which explains the greater removal efficiency of ACF-2 compared to CF. Further analysis of microbial community variability using LEfSe analysis (Fig. 6E) revealed higher LDA scores, indicating greater species variability and influence. The *Ellin6067* (LDA score: 4.107) in ACF-2 is involved in organic matter degradation and the carbon cycle [57], while *Burkholderiales* (LDA score: 4.627) contributes to electron transfer, the mineralization of DOM, and degradation of poly- and aromatic hydrocarbons [58, 59]. In contrast, the main differential genera in CF and ACF-1, such as *Nocardia* and *Gaiella* (LDA scores 4.22 and 3.904), are less effective in degrading DOM during water treatment [60]. These findings highlight that different substrate environments lead to distinct microbial communities, with ACF-2's microbial community being more efficient in removing DOM.

Figure 6

To explore the relationship between microbial diversity and the physicochemical properties of the CF/ACFs and DOM removal, Mantel analysis was performed (Fig. 7a, 7b). The results indicated significant correlations between microbial communities and factors such as microporosity (R^2 = 0.9289, p = 0.001), electrical resistance (R^2 = 0.7764, p = 0.001), and carboxyl groups (COOH) (R^2 = 0.8411, p = 0.017) of the CF/ACFs. Previous studies have shown that the electrical conductivity of materials can influence microbial community composition by altering electron-donor and electron-acceptor interactions [61]. The oxygenated functional groups on the surface of ACF enhance the adsorption of hydrophilic DOM [62], while the pore size of the packing material selectively adsorbs DOM based on molecular weight. For example, substances with molecular weights below 5 kDa, and between 5 and 10 kDa, can enter micropores and mesopores, respectively [15]. DBPFP was shown highly correlated with DOM properties (R^2 = 0.8826, p = 0.01). In addition, specific DOM characteristics were significantly correlated with microbial diversity, indicating that microbial communities contribute substantially to DOM transformation. Notably, the DOM components C1 (R^2 = 0.8235, P = 0.001) and C3 (R^2 = 0.7925, P = 0.001) showed strong correlations with microbial diversity.

Functional annotation based on PICRUSt2 predictions can reveal metabolic signatures among different systems, and the results of applying this are shown in Fig. 7c. The metabolism

pathway accounted for more than 66.5% of the ASVs across all the biofiltration systems, followed by Environmental Information Processing, Cellular Processes, and Genetic Information Processing. In terms of metabolic pathways, ACF-2 showed a greater propensity for organic matter removal and degradation compared to ACF-1, particularly in fatty acid metabolism ($P = 0.02$), the citric acid cycle ($P = 0.03$), and steroid degradation ($P = 0.02$), all of which are linked to microbial metabolism and respiration [63, 64].

Further analysis using PLS-PM indicates that the pore size distribution and surface chemical group content significantly govern microbial diversity, either directly or indirectly, thereby influencing DOM removal efficiencies (Fig. 7d). Carboxyl groups on the surface can indirectly affect microbial community structure by influencing resistivity (0.93). Previous studies have shown that microorganisms are influenced by the electron transfer process associated with the electron-conducting properties of the substrate (electrical resistance), which in turn affects microbial enrichment [65]. Additionally, the microporosity of the medium also influences microbial adaptation (1.05). The medium pore size selectively adsorbs DOM, while surface acidic functional groups play a role in DOM chemisorption [11].

Figure 7

3.7. Discussion

The results described above reveal significant differences in the physical and chemical

properties among the CF and ACFs. CF exhibits only mesopores, while ACF contains a substantial number of micropores, making it more available to LMW organic compounds (Figure 8). The adsorption capacities of ACF-1 and ACF-2 were 5 times and 6.4 times greater than that of CF, respectively. CF also has relatively fewer acidic oxygen-containing functional groups on its surface. However, medium-molecular-weight humic acids, rich in carboxyl and carbonyl groups, form hydrogen bonds with phenolic hydroxyl groups (ACF-2 > CF > ACF-1) on the medium's surface [25, 26]. This interaction results in the overlap of molecular weight distributions between CF and ACF-1. The removal efficiencies of CF for DOM and DBP precursors were only approximately 13.7% and 8%, respectively. For ACF, there are notable differences in DOM removal between ACF-1 and ACF-2, with ACF-2 achieving a 91.2% greater removal efficiency for DOM compared to ACF-1 (43.2% vs. 22.6%).

Figure 8

These significant differences can be attributed primarily to variations in microbial community structure rather than differences in physical and chemical properties. In biological filtration, microbial metabolism is often considered the main driver of organic matter degradation and the removal of other contaminants after long-term operation [66]. Microorganisms degrade or transform organic matter through secreted extracellular enzymes (e.g., proteases, amylases, cellulases), while also converting microbial metabolic activities (such as respiration or anabo-

lism) into energy and cellular substances (Figure 8). At the same time, microorganisms preferentially utilize organic matter adsorbed onto substrates, renewing the adsorption capacity and maintaining a dynamic equilibrium between microbial degradation and adsorption [15]. In short, microorganisms degrade organic matter adsorbed within the pores of the filter medium, regenerating the medium's adsorption capacity. This creates a cycle that balances biodegradation and adsorption, leading to stable removal efficiency. The dominant microbial species (*Pseudomonadota*, *Chloroflexota*, *Bacillota*) enriched in ACF-2 are beneficial for organic matter degradation and direct electron transfer mineralization. Functional analyses predict that ACF-2 is more enriched in metabolic and degradation pathways, directly contributing to its superior performance when combined with subsequent NF. This results in 78.45% removal of DOM and 83.14% and 89.6% removal of THMFP and HAAFP, respectively.

The greater capacity of ACF to remove LMW organics reduces the likelihood of NF membrane pore blockage, thus mitigating irreversible fouling-induced flux decline. Compared to CF, ACF contains a greater abundance of oxygen-containing acidic functional groups, enabling effective adsorption and removal of hydrophilic organic matter. This reduces accumulation on the NF membrane surface. Additionally, biofiltration transforms organic components by increasing their electronegativity, which enhances electrostatic repulsion with the NF membrane. This, in turn, alleviates reversible fouling and further mitigates flux decline (Figure 8). Although long-term operation may involve risks of biofilm detachment and metabolite leaching,

452 the electrochemical properties of ACF suppress leachate generation at the source by accelerat-
453 ing microbial metabolism, while efficient electron transfer also reduces the accumulation of
454 intermediate products from incomplete biodegradation. Furthermore, in NF systems, NF mem-
455 branes provide an effective physical barrier that intercepts residual leachates.

456 In conclusion, the performance of biofiltration in DOM removal is influenced by the phys-
457 ical and chemical properties of the filter media, which in turn affect microbial enrichment and
458 the microbial biodegradation rate. The combination of ACF biofiltration and NF effectively
459 removes DOM and DBPFP, while also mitigating both reversible and irreversible fouling of
460 the NF membrane, highlighting its promising application.

461

462 ## 4. Conclusion

463 The physicochemical properties of the CF determine which DOM constituents are selec-
464 tively adsorbed and jointly influence the enrichment of microbial communities. In addition, the
465 size-filtering effect and the indirect effect of carboxyl groups on the filter media's electrical
466 resistance can also influence microbial enrichment, consequently impacting the biodegradation
467 process. This biodegradation regenerates the adsorption capacity of the filter media, ultimately
468 achieving a balance between adsorption and biodegradation. The combined process of ACF
469 biofiltration and NF not only contributes to the efficient removal of DOM and DBPFP but also
470 mitigates both reversible and irreversible NF membrane fouling. This evaluation of the com-
471 bined process (ACF-based biofiltration with NF) offers valuable insights for water purification

and management, and provides a solid foundation for the practical application of the process.

CRediT authorship contribution statement

Cong Ma: Writing – review & editing; Qingqiang Dou: Investigation, Writing – original draft; Lei Xu: Conceptualization, Supervision, Writing – original draft, review & editing; Samia Saleem: Writing – review & editing; Nigel J. D. Graham: Writing – review & editing; Wen-zheng Yu: Supervision, Writing – review & editing, Funding acquisition.

Declaration of interests

The authors declare that they have no known competing financial interests or personal relationships that could have appeared to influence the work reported in this paper.

Data availability

Data will be made available on request.

Acknowledgments

This work was supported by the National Key Research and Development Program of China (Grant No. 2024YFD1700103), and the National Natural Science Foundation of China (Grant No. 52370184).

Appendix A. Supplementary data

References

[1] I.C. Iakovides, V.G. Beretsou, A. Christou, G. Gkotsis, C. Michael, T. Mina, M.-C. Nika, N.S. Thomaidis, D. Fatta-Kassinos, Impact of the wastewater treatment technology and storage on micropollutant profiles during reclaimed water irrigation: A wide-scope HRMS screening in a water-soil-lettuce-leachate system, Water Research, 279 (2025) 123319.

[2] E. Helte, M. Save-Soderbergh, H. Ugge, K. Fall, A. Akesson, S.C. Larsson, Chlorination by-products in drinking water and risk of bladder cancer - A population-based cohort study, Water Research, 214 (2022) 118202.

[3] F. Wang, J. Yin, X. Wang, H. Zhang, Y. Song, X. Zhang, T. Wang, Exposure to trichloromethane via drinking water promotes progression of colorectal cancer by activating IRE1α/XBP1 pathway of endoplasmic reticulum stress, Science of The Total Environment, 949 (2024) 175040.

[4] R. Nabaterega, R.N. Vesuwe, O.T. Iorhemen, Statistical evaluation of different filter media and application of multiple criteria analysis to select the best media for pollutants removal in wastewater biofiltration: A review, Science of The Total Environment, 996 (2025) 180104.

[5] M. Yaqub, W. Lee, Comparison of different activated carbon fibers for natural organic matter removal from lake water, Desalination and Water Treatment, 184 (2020) 130-138.

[6] H. Fallou, N. Cimetière, S. Giraudet, D. Wolbert, P. Le Cloirec, Adsorption of pharmaceuticals onto activated carbon fiber cloths – Modeling and extrapolation of adsorption isotherms at very low concentrations, Journal of Environmental Management, 166 (2016) 544-555.

[7] W. Tang, P. Zhang, J. Xia, X. Zeng, Kinetics of manganese removal from groundwater via biological activated carbon fiber, 22 (2024) 1171-1181.

[8] Z.D. Lu, Z.B. Jing, J. Huang, Y.C. Ke, C. Li, Z.N. Zhao, X.W. Ao, W.J. Sun, Can we shape microbial communities to enhance biological activated carbon filter performance?, Water Research, 212 (2022) 118104.

[9] Z.D. Lu, C. Li, Z.B. Jing, X.W. Ao, Z.Y. Chen, W.J. Sun, Implication on selection and replacement of granular activated carbon used in biologically activated carbon filters through meta-omics analysis, Water Research, 198 (2021) 117152.

[10] Y. Zhang, C.C. Wayner, S. Wu, X. Liu, W.P. Ball, S.P. Preheim, Effect of Strain-Specific Biofilm Properties on the Retention of Colloids in Saturated Porous Media under Conditions of Stormwater Biofiltration, Environmental Science & Technology, 55 (2021) 2585-2596.

[11] A. Hu, M. Choi, A.J. Tanentzap, J. Liu, K.-S. Jang, J.T. Lennon, Y. Liu, J. Soininen, X. Lu, Y. Zhang, J. Shen, J. Wang, Ecological networks of dissolved organic matter and microorganisms under global change, Nature Communications, 13 (2022) 3600.

[12] D.B. Mosqueda-Jimenez, P.M. Huck, Effect of biofiltration as pretreatment on the fouling of nanofiltration membranes, Desalination, 245 (2009) 60-72.

[13] S.L. Goertzen, K.D. Thériault, A.M. Oickle, A.C. Tarasuk, H.A. Andreas,

533 Standardization of the Boehm titration. Part I. CO_2 expulsion and endpoint determination,
534 Carbon, 48 (2010) 1252-1261.
535 [14] J. Yuan, E. Passeport, R. Hofmann, Understanding adsorption and biodegradation in
536 granular activated carbon for drinking water treatment: A critical review, Water Research, 210
537 (2022) 118026.
538 [15] Z. Lu, W. Sun, C. Li, W. Cao, Z. Jing, S. Li, X. Ao, C. Chen, S. Liu, Effect of granular
539 activated carbon pore-size distribution on biological activated carbon filter performance, Water
540 Research, 177 (2020) 115768.
541 [16] N.-K. Kim, S. Oh, W.-T. Liu, Enrichment and characterization of microbial consortia
542 degrading soluble microbial products discharged from anaerobic methanogenic bioreactors,
543 Water Research, 90 (2016) 395-404.
544 [17] B. Siembida-Lösch, W.B. Anderson, Y. Wang, J. Bonsteel, P.M. Huck, Effect of ozone
545 on biopolymers in biofiltration and ultrafiltration processes, Water Research, 70 (2015) 224-
546 234.
547 [18] H. Lin, L. Guo, Variations in Colloidal DOM Composition with Molecular Weight
548 within Individual Water Samples as Characterized by Flow Field-Flow Fractionation and EEM-
549 PARAFAC Analysis, Environmental Science & Technology, 54 (2020) 1657-1667.
550 [19] K.R. Murphy, A. Hambly, S. Singh, R.K. Henderson, A. Baker, R. Stuetz, S.J. Khan,
551 Organic Matter Fluorescence in Municipal Water Recycling Schemes: Toward a Unified
552 PARAFAC Model, Environmental Science & Technology, 45 (2011) 2909-2916.
553 [20] L. Tian, P. Zhou, Z. Su, T. Liu, N. Graham, T. Bond, W. Yu, Insights into the properties
554 of surface waters and their associated nanofiltration membrane fouling: The importance of
555 biopolymers and high molecular weight humics, Chemical Engineering Journal, 451 (2023)
556 138682.
557 [21] Y. Yamashita, J.N. Boyer, R. Jaffé, Evaluating the distribution of terrestrial dissolved
558 organic matter in a complex coastal ecosystem using fluorescence spectroscopy, Continental
559 Shelf Research, 66 (2013) 136-144.
560 [22] A.-R. Schittich, U.J. Wünsch, H.V. Kulkarni, M. Battistel, H. Bregnhøj, C.A.
561 Stedmon, U.S. McKnight, Investigating Fluorescent Organic-Matter Composition as a Key
562 Predictor for Arsenic Mobility in Groundwater Aquifers, Environmental Science & Technology,
563 52 (2018) 13027-13036.
564 [23] S. Chen, Y. Lu, P. Dash, P. Das, J. Li, K. Capps, H. Majidzadeh, M. Elliott, Hurricane
565 pulses: Small watershed exports of dissolved nutrients and organic matter during large storms
566 in the Southeastern USA, Science of The Total Environment, 689 (2019) 232-244.
567 [24] Z. Wang, Z. Xu, Y. Guan, H. Zhu, G. Yuan, Z. Dong, X. Li, Q. Zhang, Y. Cong,
568 Preparation of pitch-based activated carbon fibers with high specific surface area and excellent
569 adsorption properties, Research on Chemical Intermediates, 48 (2022) 1733-1746.
570 [25] Y. Liang, J. He, S. Zhang, T. Lao, Influence of different relative molecular masses of
571 DOM on the adsorption of carbamazepine by quartz sand, Acta Petrologica et Mineralogica,
572 37 (2018) 975-984.
573 [26] A. Ahmad, N. Martsinovich, Atomic-scale modelling of organic matter in soil:

574 adsorption of organic molecules and biopolymers on the hydroxylated α-Al_2O_3 (0001) surface,
575 Philosophical Transactions of the Royal Society a-Mathematical Physical and Engineering
576 Sciences, 381 (2023) 2250.
577 [27] M.M. Taimur Khan, S. Takizawa, Z. Lewandowski, M. Habibur Rahman, K.
578 Komatsu, S.E. Nelson, F. Kurisu, A.K. Camper, H. Katayama, S. Ohgaki, Combined effects of
579 EPS and HRT enhanced biofouling on a submerged and hybrid PAC-MF membrane bioreactor,
580 Water Research, 47 (2013) 747-757.
581 [28] J. Feng, X. Li, Y. Yang, X. Fan, Z. Zhou, J. Ren, X. Tan, H. Li, Insight into biofouling
582 mechanism in biofiltration-facilitated gravity-driven membrane (GDM) system: Beneficial
583 effects of pre-deposited adsorbents, Journal of Membrane Science, 662 (2022) 121017.
584 [29] L. Xu, Z. Zhou, N.J.D. Graham, M.J. Liu, W.Z. Yu, Enhancing ultrafiltration
585 performance by gravity-driven up-flow slow biofilter pre-treatment to remove natural organic
586 matters and biopolymer foulants, Water Research, 195 (2021) 117010.
587 [30] B.-B. Wang, X.-T. Liu, J.-M. Chen, D.-C. Peng, F. He, Composition and functional
588 group characterization of extracellular polymeric substances (EPS) in activated sludge: the
589 impacts of polymerization degree of proteinaceous substrates, Water Research, 129 (2018) 133-
590 142.
591 [31] U. Hübner, D. Wolff, S. Achermann, J.E. Drewes, A. Wick, K. Fenner, Analyzing
592 (Initial) Biotransformation Reactions as an Organizing Principle for Unraveling the Extent of
593 Trace Organic Chemical Biotransformation in Biofiltration Systems, Acs Es&T Water, 1 (2021)
594 1921-1931.
595 [32] M. Hasan, K. Alfredo, S. Murthy, R. Riffat, Biodegradation of salicylic acid,
596 acetaminophen and ibuprofen by bacteria collected from a full-scale drinking water biofilter,
597 Journal of Environmental Management, 295 (2021) 113071.
598 [33] L. Wang, W. Weng, N. Graham, W. Yu, K. Sun, T. Liu, Biopolymers present in tap
599 water improve disinfection byproduct removal by nanofiltration, Separation and Purification
600 Technology, 362 (2025) 131718.
601 [34] M. Park, T. Anumol, J. Simon, F. Zraick, S.A. Snyder, Pre-ozonation for high
602 recovery of nanofiltration (NF) membrane system: Membrane fouling reduction and trace
603 organic compound attenuation, Journal of Membrane Science, 523 (2017) 255-263.
604 [35] W.Z. Yu, T. Liu, J. Crawshaw, T. Liu, N. Graham, Ultrafiltration and nanofiltration
605 membrane fouling by natural organic matter: Mechanisms and mitigation by pre-ozonation and
606 pH, Water Res., 139 (2018) 353-362.
607 [36] M.A. Zazouli, H. Susanto, S. Nasseri, M. Ulbricht, Influences of solution chemistry
608 and polymeric natural organic matter on the removal of aquatic pharmaceutical residuals by
609 nanofiltration, Water Research, 43 (2009) 3270-3280.
610 [37] D. Yadav, S. Karki, P.G. Ingole, Current advances and opportunities in the
611 development of nanofiltration (NF) membranes in the area of wastewater treatment, water
612 desalination, biotechnological and pharmaceutical applications, Journal of Environmental
613 Chemical Engineering, 10 (2022) 108109.
614 [38] Y.-A. Boussouga, M.B. Mohankumar, A. Gopalakrishnan, A. Welle, A.I. Schäfer,

615 Removal of arsenic(III) via nanofiltration: contribution of organic matter interactions, Water
616 Research, 201 (2021) 117315.
617 [39] D.S. Mallya, S. Abdikheibari, L.F. Dumée, S. Muthukumaran, W. Lei, K. Baskaran,
618 Removal of natural organic matter from surface water sources by nanofiltration and surface
619 engineering membranes for fouling mitigation – A review, Chemosphere, 321 (2023) 138070.
620 [40] W. Yu, T. Liu, J. Crawshaw, T. Liu, N. Graham, Ultrafiltration and nanofiltration
621 membrane fouling by natural organic matter: Mechanisms and mitigation by pre-ozonation and
622 pH, Water Research, 139 (2018) 353-362.
623 [41] A.W. Zularisam, A.F. Ismail, M.R. Salim, M. Sakinah, H. Ozaki, The effects of
624 natural organic matter (NOM) fractions on fouling characteristics and flux recovery of
625 ultrafiltration membranes, Desalination, 212 (2007) 191-208.
626 [42] K. Chon, S. Sarp, S. Lee, J.-H. Lee, J.A. Lopez-Ramirez, J. Cho, Evaluation of a
627 membrane bioreactor and nanofiltration for municipal wastewater reclamation: Trace
628 contaminant control and fouling mitigation, Desalination, 272 (2011) 128-134.
629 [43] H. Yamamura, K. Okimoto, K. Kimura, Y. Watanabe, Hydrophilic fraction of natural
630 organic matter causing irreversible fouling of microfiltration and ultrafiltration membranes,
631 Water Research, 54 (2014) 123-136.
632 [44] F. Hammes, E. Salhi, O. Koster, H.P. Kaiser, T. Egli, U. von Gunten, Mechanistic and
633 kinetic evaluation of organic disinfection by-product and assimilable organic carbon (AOC)
634 formation during the ozonation of drinking water, Water Res, 40 (2006) 2275-2286.
635 [45] X. Mao, N.Y. Xu, X.Y. Shi, H. Wen, C.K. Liu, Integration of charge repulsion and
636 size exclusion effects into the skin layer matrix for enhanced Mg^{2+}/Li^{+} nanofiltration separation,
637 Journal of Membrane Science, 713 (2025) 123315.
638 [46] M. Thanuttamavong, K. Yamamoto, J.I. Oh, K.H. Choo, S.J. Choi, Rejection
639 characteristics of organic and inorganic pollutants by ultra low-pressure nanofiltration of
640 surface water for drinking water treatment, Desalination, 145 (2002) 257-264.
641 [47] H.-C. Kim, M.-J. Yu, Characterization of natural organic matter in conventional water
642 treatment processes for selection of treatment processes focused on DBPs control, Water
643 Research, 39 (2005) 4779-4789.
644 [48] N. Sharma, S. Mohapatra, L.P. Padhye, S. Mukherji, Role of precursors in the
645 formation of trihalomethanes during chlorination of drinking water and wastewater effluents
646 from a metropolitan region in western India, Journal of Water Process Engineering, 40 (2021)
647 101928.
648 [49] D.T. Scott, D.M. McKnight, E.L. Blunt-Harris, S.E. Kolesar, D.R. Lovley, Quinone
649 Moieties Act as Electron Acceptors in the Reduction of Humic Substances by Humics-
650 Reducing Microorganisms, Environmental Science & Technology, 32 (1998) 2984-2989.
651 [50] X. Liu, H. Qin, S. Xing, Y. Liu, C. Chu, D. Yang, X. Duan, S. Mao, Selective Removal
652 of Organic Pollutants in Groundwater and Surface Water by Persulfate-Assisted Advanced
653 Oxidation: The Role of Electron-Donating Capacity, Environmental Science & Technology, 57
654 (2023) 13710-13720.
655 [51] W.A. Mitch, S.D. Richardson, X.R. Zhang, M. Gonsior, High-molecular-weight by-

products of chlorine disinfection, Nature Water, 1 (2023) 336-347.
[52] Z. Tang, D. Xie, S. Li, L. Huang, The directions of enhanced activated carbon fibers for iodine capture from humid gas streams: Synergistic mechanisms of microporosity, hydrophobicity, and nitrogen sites, Separation and Purification Technology, 354 (2025) 129032.
[53] Y. Han, Y. Luo, L. Zhang, X. Lu, X. Luo, X. Wu, F. Zan, Deciphering the mechanistic insight into modified biochar for distinct anaerobic digestion processes: Surface functional groups and electron-transmitting capabilities, Journal of Environmental Chemical Engineering, 13 (2025) 115581.
[54] X. Wang, J. Li, J. Zheng, L. Zhao, C. Ruan, D. Zhang, X. Pan, Polysaccharide preferred minority-dominant community assembly and exoenzyme enrichment in transparent exopolymer particles: Implication for global carbon cycle in water, Science of The Total Environment, 914 (2024) 169976.
[55] L.B.M. Speirs, D.T.F. Rice, S. Petrovski, R.J. Seviour, The Phylogeny, Biodiversity, and Ecology of the Chloroflexi in Activated Sludge Frontiers in Microbiology, 10 (2019) 2015.
[56] F. Chai, L. Li, S. Xue, J. Liu, Auxiliary voltage enhanced microbial methane oxidation co-driven by nitrite and sulfate reduction, Chemosphere, 250 (2020) 126259.
[57] X. Wang, Z. Zhang, X. Yang, Y. Wang, Y. Li, T. Zhu, Y. Zhao, B.-J. Ni, Y. Liu, Interaction of poly dimethyl diallyl ammonium chloride with sludge components: Anaerobic digestion performance and adaptive changes of anaerobic microbes, Water Research, 266 (2024) 122368.
[58] Y. Li, H.-M. Zhang, Calcined pyrite accelerates sulfur metabolic and electron transfer in driving targeted microbial fuel cell denitrification, Bioresource Technology, 410 (2024) 131285.
[59] R.M. Niemi, I. Heiskanen, R. Heine, J. Rapala, Previously uncultured β-Proteobacteria dominate in biologically active granular activated carbon (BAC) filters, Water Research, 43 (2009) 5075-5086.
[60] S.Y. Zhang, T.T. Cui, X.W. Liu, M.J. Zhan, X. Song, Y. Xu, R. Yu, Sludge biolysis pretreatment to reduce antibiotic resistance genes (ARGs): Insight into the relationship between potential ARGs hosts and BALOs' preferred prey, Water Research, 260 (2024) 121949.
[61] H. Liu, Y. Xu, X. Dai, Electron-transfer-driven spatial optimisation of anaerobic consortia for efficient methanogenesis: Neglected inductive effect of conductive materials, Bioresource Technology, 403 (2024) 130856.
[62] T. Karanfil, J.E. Kilduff, Role of granular activated carbon surface chemistry on the adsorption of organic compounds. 1. Priority pollutants (vol 33, pg 3217, 1999), Environmental Science & Technology, 34 (2000) 2372-2372.
[63] W. Yang, Y. Liang, T. Li, W. Li, X. Liao, B. Wang, X. Wang, S. Wang, Interactions between iron mineral and low-molecular-weight organic acids accelerated nitrogen conversion and release in lake sediments, Water Research, 275 (2025) 123174.
[64] T. Rosenqvist, J. Hilding, C. Suarez, C.J. Paul, Microbial communities in slow sand filters for drinking water treatment adapt to organic matter altered by ozonation, Water Research, 270 (2025) 122843.

[65] Z. Hao, Q. Wang, Z. Yan, H. Jiang, Novel magnetic loofah sponge biochar enhancing microbial responses for the remediation of polycyclic aromatic hydrocarbons-contaminated sediment, Journal of Hazardous Materials, 401 (2021) 123859.

[66] L.C. Wei, J.J. Zheng, Y.T. Han, X.Y. Xu, M.Y. Li, L. Zhu, Insights into the roles of biochar pores toward alleviating antibiotic resistance genes accumulation in biofiltration systems, Bioresource Technology, 394 (2024) 130257.

Figure Captions

Figure 1. Water quality characteristics during operation of biofilters: (a) DOC concentrations in the influent and effluents, and corresponding DOC removal rates; (b) DOM fluorescence characteristics of the water samples during Stage II, as identified by PARAFAC analysis; and (c) Changes in the abundance of the three fluorescent components (C1, C2, C3) in different water samples during Stage II.

Figure 2. (a) MW distribution of DOM in raw water and effluents from the different biofilters; (b) Quantification of DOM fractions within different MW ranges; (c) Changes in the content of microbially-derived biopolymers; and (d) Integral quantification of EEM fluorescence regions in raw water and biofilter effluents.

Figure 3. (a) High-resolution C 1s and O 1s XPS spectra of DOM in raw water and effluents from the different biofilters; (b) Normalized flux during NF tests; (c) Schematic diagram illustrating DOM retention by the NF membrane; and (d) Water contact angles of virgin and air-dried fouled NF membranes after filtration.

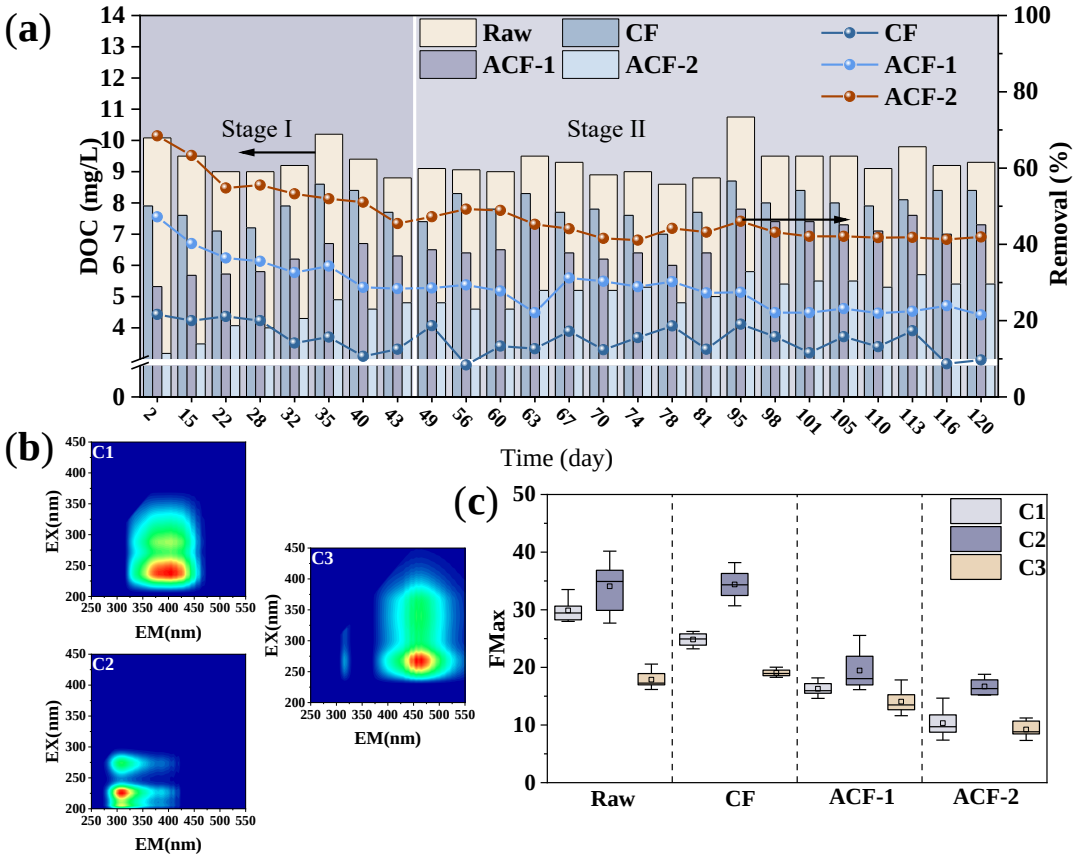
Figure 4. Water quality analysis before and after NF: (a) DOC concentrations before and after NF, using raw water or biofilter effluents as the feed solution; (b) EEM fluorescence spectra of different NF effluents; (c) MW distribution of raw water and different NF effluents; and (d) DBPFP of water samples before and after NF.

Figure 5. Physicochemical properties of the CF and ACFs: (a) N_2 adsorption/desorption isotherms of the ACFs; (b) Pore volume and specific surface area; (c) Pseudo-second-order adsorption kinetics of DOM onto the CF and ACFs; (d) Surface acidic functional group content; and (e) High-resolution C 1s XPS spectra of the CF and ACFs.

Figure 6. Microbial community structure analysis: (a) Principal coordinate analysis (PCoA) plot based on Bray-Curtis dissimilarity of ASVs; (b) Venn diagram showing shared and unique ASVs among the three biofilters; (c) Alpha-diversity of the microbial communities (Chao1 and Shannon indices); (d) Relative abundance of dominant bacterial phyla; and (e) LEfSe analysis identifying significantly enriched bacteria in each biofilter ($p < 0.05$, LDA score > 4).

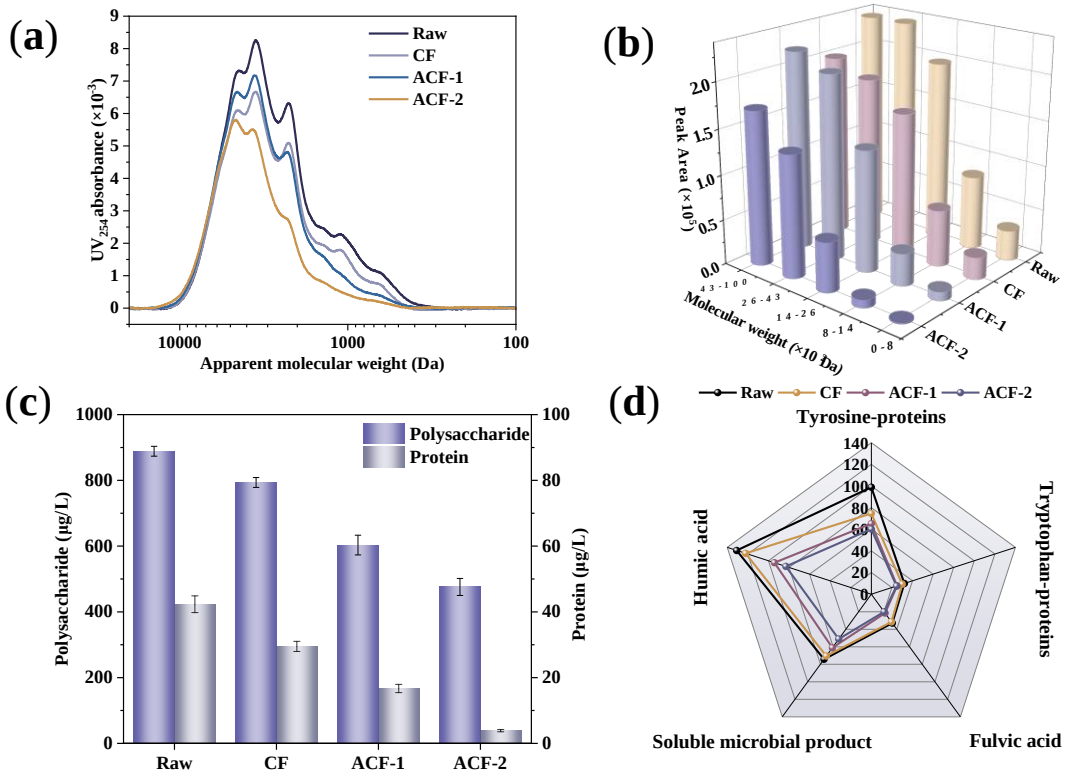
Figure 7. Correlation and functional analyses: (a) Relationships among microbial composition, DOM characteristics, and CF properties; (b) Impact of DOM characteristics on microbial composition; (c) Extended error bar plot of predicted functional pathways (KEGG Level 3) with significantly different abundances in ACF-1 and ACF-2 (FDR-adjusted $p < 0.05$); and (d) PLS-PM analysis showing how the pore size distribution and surface chemical groups of the ACFs govern microbial diversity and DOM removal (red lines = positive correlation; blue lines = negative correlation; The black line represents aspects that are not directly related to the PLS-PM, but are part of the overall mechanism for DOM degradation.).

738 **Figure 8.** Schematic diagram illustrating the mechanisms of DOM removal by ACF biofiltra-
739 tion and the subsequent impacts on NF fouling.



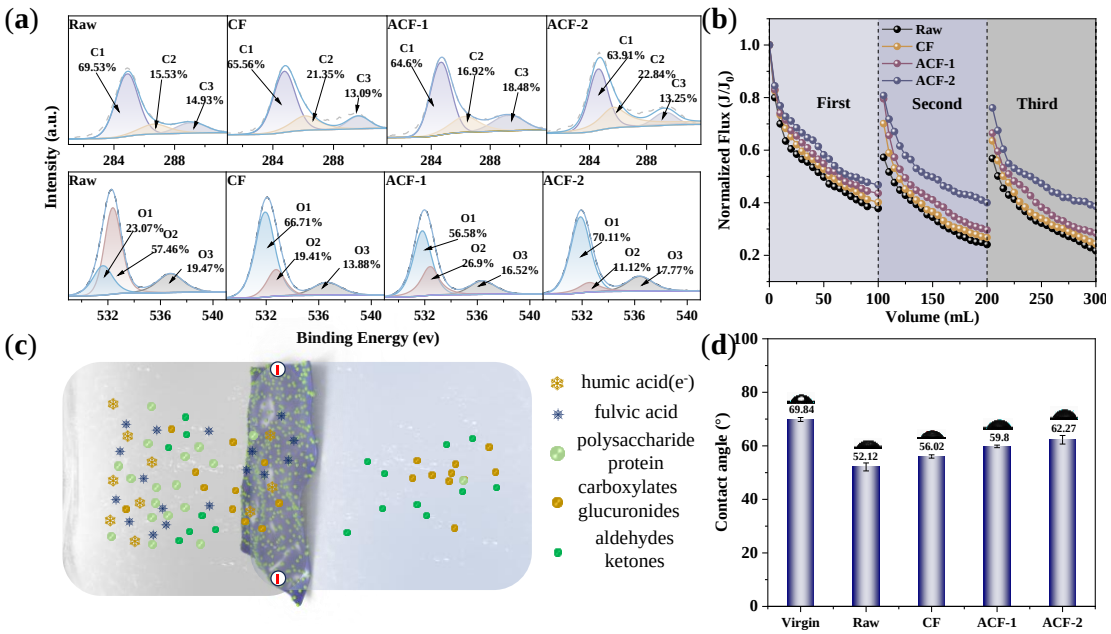
740

741 **Figure 1.** Water quality characteristics during operation of biofilters: (a) DOC concentrations
742 in the influent and effluents, and corresponding DOC removal rates; (b) DOM fluorescence
743 characteristics of the water samples during Stage II, as identified by PARAFAC analysis; and
744 (c) Changes in the abundance of the three fluorescent components (C1, C2, C3) in different
745 water samples during Stage II.



746

747 **Figure 2.** (a) MW distribution of DOM in raw water and effluents from the different biofilters;
748 (b) Quantification of DOM fractions within different MW ranges; (c) Changes in the content
749 of microbially-derived biopolymers; and (d) Integral quantification of EEM fluorescence re-
750 gions in raw water and biofilter effluents.



751

752 **Figure 3.** (a) High-resolution C 1s and O 1s XPS spectra of DOM in raw water and effluents
753 from the different biofilters; (b) Normalized flux during NF tests; (c) Schematic diagram illus-
754 trating DOM retention by the NF membrane; and (d) Water contact angles of virgin and air-
755 dried fouled NF membranes after filtration.

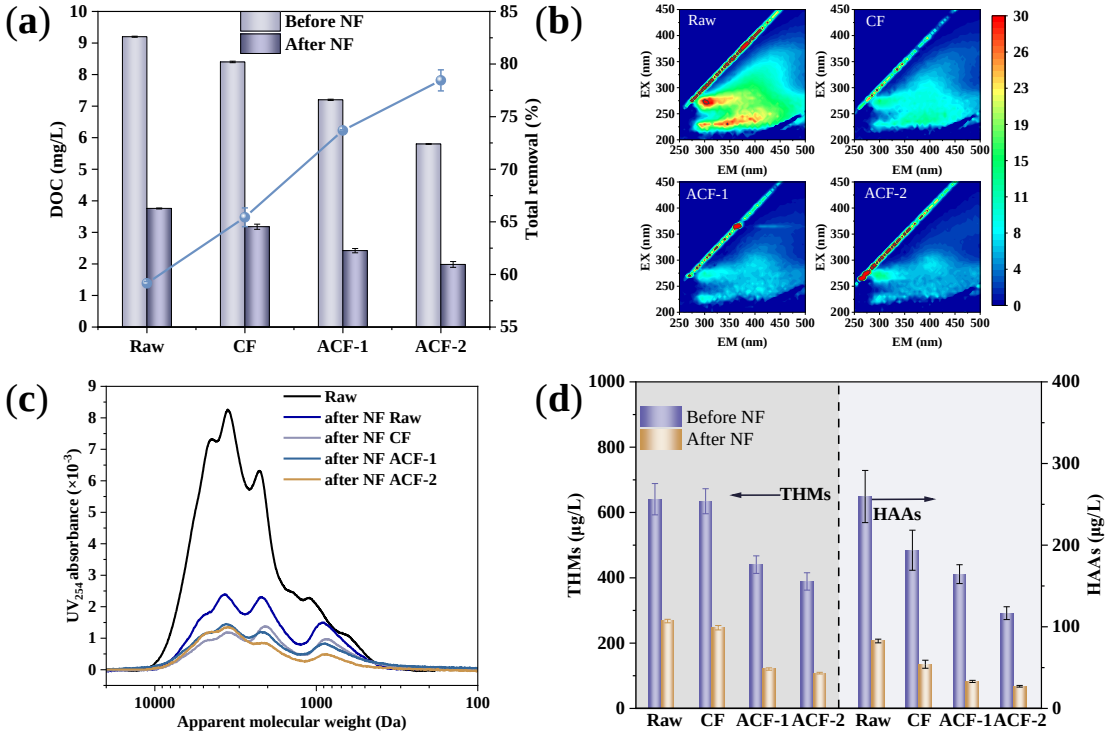
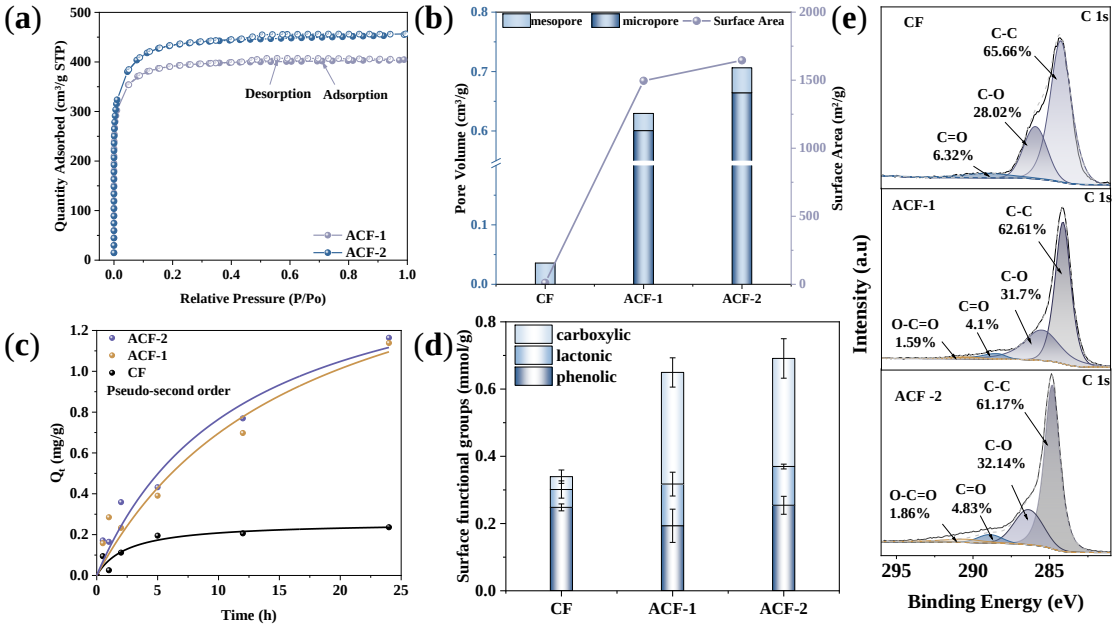
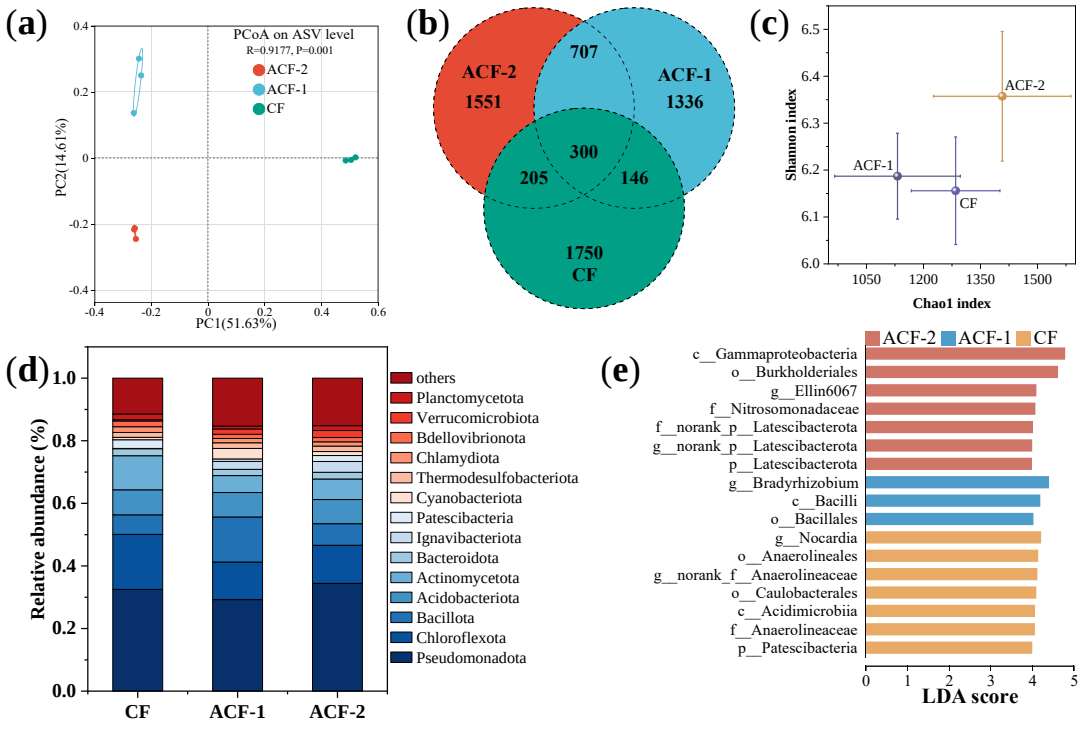


Figure 4. Water quality analysis before and after NF: (a) DOC concentrations before and after NF, using raw water or biofilter effluents as the feed solution; (b) EEM fluorescence spectra of different NF effluents; (c) MW distribution of raw water and different NF effluents; and (d) DBPFP of water samples before and after NF.



761

762 **Figure 5.** Physicochemical properties of the CF and ACFs: (a) N_2 adsorption/desorption iso-
763 therms of the ACFs; (b) Pore volume and specific surface area; (c) Pseudo-second-order ad-
764 sorption kinetics of DOM onto the CF and ACFs; (d) Surface acidic functional group content;
765 and (e) High-resolution C 1s XPS spectra of the CF and ACFs.



766

767 **Figure 6.** Microbial community structure analysis: (a) Principal coordinate analysis (PCoA)
768 plot based on Bray-Curtis dissimilarity of ASVs; (b) Venn diagram showing shared and unique
769 ASVs among the three biofilters; (c) Alpha-diversity of the microbial communities (Chao1 and
770 Shannon indices); (d) Relative abundance of dominant bacterial phyla; and (e) LEfSe analysis
771 identifying significantly enriched bacteria in each biofilter ($p < 0.05$, LDA score > 4).

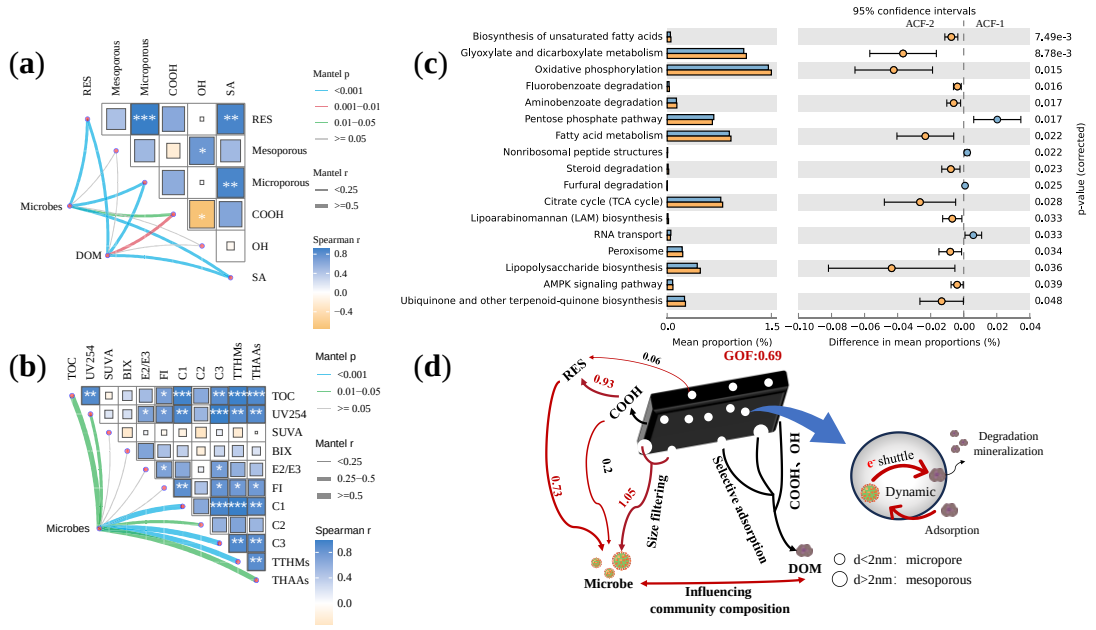
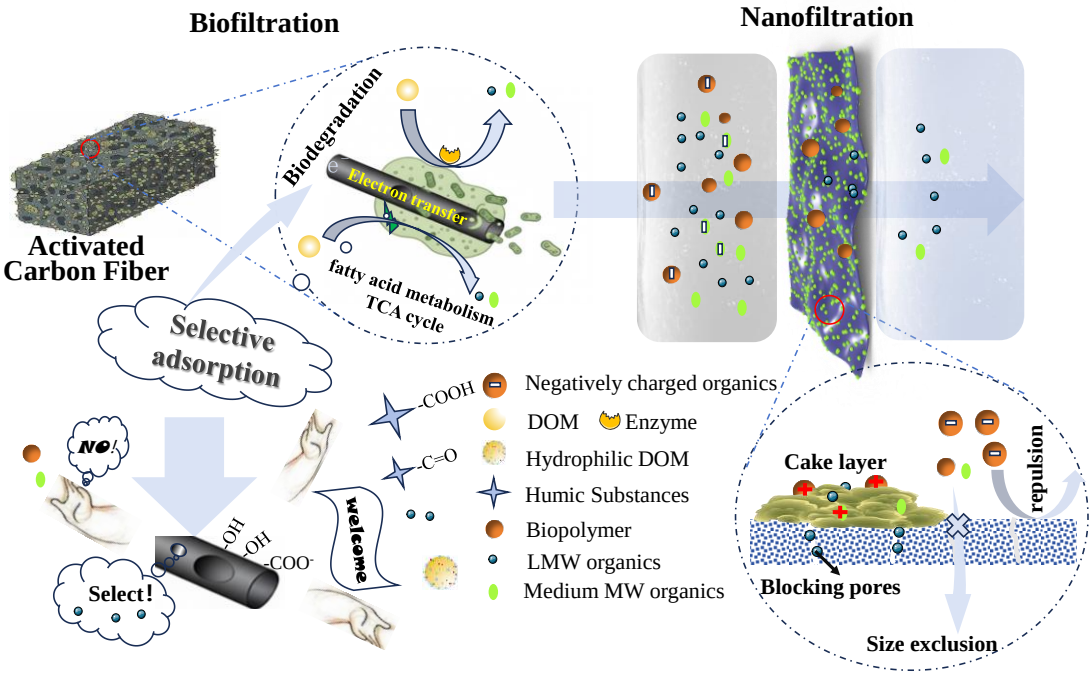


Figure 7. Correlation and functional analyses: (a) Relationships among microbial composition, DOM characteristics, and CF properties; (b) Impact of DOM characteristics on microbial composition; (c) Extended error bar plot of predicted functional pathways (KEGG Level 3) with significantly different abundances in ACF-1 and ACF-2 (FDR-adjusted $p < 0.05$); and (d) PLS-PM analysis showing how the pore size distribution and surface chemical groups of the ACFs govern microbial diversity and DOM removal (red lines = positive correlation; blue lines = negative correlation; The black line represents aspects that are not directly related to the PLS-PM, but are part of the overall mechanism for DOM degradation.).



781

782 **Figure 8.** Schematic diagram illustrating the mechanisms of DOM removal by ACF biofiltra-
783 tion and the subsequent impacts on NF fouling.